POLITECNICO DI TORINO
Repository ISTITUZIONALE

La Cappella Reale nella chiesa della Confraternita dello Spirito Santo in Govone

Original
La Cappella Reale nella chiesa della Confraternita dello Spirito Santo in Govone / Gianasso, E. (HEREDIUM). - In: Da insediamento fortificato a Reale Villeggiatura. Committenza, architettura e paesaggio per il castello di Govone / Malvicino L.. - STAMPA. - Sesto Fiorentino : All'Insegna del Giglio, 2023. - ISBN 9788892851597. - pp. 331-340 [10.36153/heredium04-050]

Availability:
This version is available at: 11583/2980491 since: 2023-07-18T17:52:20Z

Publisher:
All'Insegna del Giglio

Published
DOI:10.36153/heredium04-050

Terms of use:

This article is made available under terms and conditions as specified in the corresponding bibliographic description in the repository

Publisher copyright

(Article begins on next page)

13 October 2026

ADVANCED MATERIALS INTERFACES
Open Access
www.advmatinterfaces.de

Check for updates

Durable Bio-Based Nanocomposite Coating on Urinary Catheters Prevents Early-Stage CAUTI-Associated Pathogenicity

*Antonio Puertas-Segura, Kristina Ivanova, Leonardo Martín Pérez, Bzazou El Ouazzani Zine El Abidine, Aleksandra Ivanova, Barış Gökalsın, Gianluca Ciardelli, and Tzanko Tzanov**

Recurrent catheter-associated urinary tract infections (CAUTIs) in catheterized patients, increase their morbidity and hospital stay at substantial costs for healthcare systems. Hence, novel and efficient strategies for mitigating CAUTIs are needed. In this work, a bio-based nanocomposite coating is engineered with bactericidal, antibiofilm, and antioxidant properties on commercial silicone catheters using a combined ultrasound/nanoparticles (NPs) driven coating approach. This approach integrates citronellal-loaded lauryl gallate NPs (CLG_NPs), as both antimicrobial and structural elements, with chitosan (CS), in a substrate-independent sonochemical coating process. The hybrid CS/CLG_NPs coating shows pH-dependent citronellal release, strong antibacterial activity toward the common CAUTI pathogens *Escherichia coli* and *Staphylococcus aureus*, alongside strong antioxidant activity, and biocompatibility to fibroblast and keratinocytes. Moreover, the nano-enabled coating significantly mitigated bacterial biofilm formation after a week in a simulated human bladder environment, outperforming the commercially-available silicone catheters. These results underscore the potential of the novel biopolymer nanocomposites obtained by ultrasound coating technology, offering a straightforward antimicrobial/antibiofilm solution for indwelling medical devices.

1. Introduction

Catheter-associated urinary tract infections (CAUTIs) are prevalent (more than 75%) over other infections in hospitalized patients.[1] Indwelling catheters facilitate the entrance of microbes into the bladder which leads to the development of hard-to-treat urinary infections, as well as catheter malfunctioning. For instance, extraluminal colonization by the rich periurethral flora occurs upon catheter insertion, or later by microbes ascending along the catheter-urethra interface. Therefore, even closed drainage systems and aseptic care cannot prevent bacteriuria. Each successive day of catheterization increases by ≈3–10% the risk of acquiring persistent microbial infection. CAUTIs require intensive antibiotic therapies resulting in patient discomfort, prolonged hospitalization, and a substantial economic burden for the healthcare system,[2,3] besides promoting antimicrobial resistance (AMR). Biofilms on the catheters provide an optimal environment for microbial gene transfer[4] and further ease the AMR acquisition. Therefore, the development and validation of efficient strategies for reducing CAUTIs are a continuing challenge for device manufacturers. In this regard, replacing latex as a material for the production of catheters with silicone derivatives with reduced susceptibility to bacterial adhesion has proven to be

A. Puertas-Segura, K. Ivanova, L. M. Pérez, A. Ivanova, T. Tzanov
Grup de Biotecnologia Molecular i Industrial
Department of Chemical Engineering
Universitat Politècnica de Catalunya
Terrassa, Spain
E-mail: tzanko.tzanov@upc.edu

The ORCID identification number(s) for the author(s) of this article can be found under https://doi.org/10.1002/admi.202401016

© 2025 The Author(s). Advanced Materials Interfaces published by Wiley-VCH GmbH. This is an open access article under the terms of the Creative Commons Attribution License, which permits use, distribution and reproduction in any medium, provided the original work is properly cited.

DOI: 10.1002/admi.202401016

B. E. O. Z. E. Abidine
Biotechnological Valorization of Microorganisms Laboratory
Department of Life Science
Abdelmalek Essaadi University
Tangier, Morocco

B. Gökalsın
Departament of Biology
Marmara University
Istanbul, Turkey

G. Ciardelli
Department of Mechanical and Aerospace Engineering
Politecnico di Torino
Torino, Italy

ineffective.[5] Currently, the most promising strategies to prevent biofilm formation on catheters, which have not yet been adopted industrially, are based on nanostructured coatings.[6] Among these, ultrasound-assisted coating technology has emerged as one of the most straightforward tools for the functionalization of catheters, upvoted by IUPAC as a top-ten emerging technology in 2021.[7] This surface nano-enabling technology is rapid, cost-effective, scalable, and environmentally sustainable. It is water-based, operates at low temperatures, and provides durable, ready-to-use surface nanostructured products.[8] We employed the ultrasound-assisted process to develop different coatings based on polymers, peptides, enzymes, metal, and hybrid metal-biopolymer nanoparticles (NPs) to enhance the infection-free lifespan of silicone catheters.[8–10] Unlike metal NPs, which may pose human and environmental toxicity concerns, essential oils (EOs) are natural, biodegradable, and generally non-toxic at therapeutic doses. EOs demonstrated strong antibacterial and antibiofilm efficacy against both Gram-positive and Gram-negative bacteria, including those implicated in CAUTIs,[11–13] while effectively circumventing the development of AMR.[14] However, the inherent volatility and poor water solubility of EOs preclude their use in direct clinical applications. To overcome these challenges, nanoencapsulation laid out an effective solution for improved stability, bactericidal activity, and controlled release of EOs,[15–17] although the use of nanoformulated EOs for catheter functionalization is scarcely reported.[18]

In this work, we engineered bio-based nanocomposite coatings using citronellal-loaded lauryl gallate NPs (CLG_NPs) acting as both multifunctional (antibacterial, antibiofilm, and antioxidant) and structural components, embedded in a chitosan matrix on silicone catheters upon application of high-intensity ultrasound (US). The proven anti-inflammatory, antimicrobial, and antioxidant properties of citronellal, the principal active of citronella oil, account for its wide use in different medical applications.[19] The choice of an ester derivative of gallic acid, lauryl gallate (LG), for citronellal encapsulation is based on its ability to stabilize hydrophobic molecules by hydrophobic interactions, enable controlled actives release, and synergistically boost antimicrobial and antioxidant efficiency at lower, non-toxic concentrations.[20,21] Furthermore, lauryl gallate forms phenolic shell vesicles that promote interfacial interaction and self-assembly with amino and hydroxyl groups of chitosan, emulating the mechanism of mussel-inspired adhesion.[22] This interaction will be further enhanced by the ultrasound treatment, which will improve the mass transfer and ensure coating attachment to the otherwise inert catheter surface. Therefore, we first produced stable CLG_NPs by ultrasonic nanoemulsification approach and used them together with chitosan to coat sonochemically polydimethylsiloxane (PDMS) catheters without any material pre-activation. The successful deposition of the hybrid CS/CLG_NPs coating was confirmed by atomic force microscopy (AFM), confocal microscopy, and contact angle measurements. The antimicrobial and antibiofilm properties of the coated catheters were tested against the prevalent biofilm-forming CAUTI-associated pathogens *Staphylococcus aureus* and *Escherichia coli* in a lab model of the human bladder for up to 7 days, matching the timeframe for initial catheter colonization by pathogens and infection occurrence.[23] Additionally, the stability of the nanocomposite coating was assessed within the typical pH range for normal urine by monitoring the release of citronellal using high-performance liquid chromatography (HPLC). Finally, the biocompatibility of CS/CLG_NPs-coated catheters was validated in vitro using human fibroblasts and keratinocytes due to their essential roles in the architecture of bladder mucosa and epithelial layer, respectively.

2. Experimental Section

2.1. Materials

Polydimethylsiloxane (PDMS) flat sheets and urinary catheters were supplied by Degania Silicone Ltd. (Israel). Lauryl gallate, citronellal, tween 80, low molecular weight chitosan, Baird-Parker agar, Coliform ChromoSelect agar, Luria-Bertani (LB) broth, agar powder, nutrient broth (NB), N-acetyl homoserine lactone (AHL), phosphate-buffered saline (PBS), sodium dodecyl sulfate (SDS), Nile red, fluorescein isocyanate (FITC), crystal violet, 2,2-diphenyl-1-picrylhydrazyl (DPPH) and Dulbecco's modified Eagle's medium (DMEM) were purchased from Sigma–Aldrich (Spain). Ethanol was purchased from Scharlab (Spain). Alamar Blue cell viability reagent and Live/Dead BacLight kit were obtained from Invitrogen (Spain). *Staphylococcus aureus* (ATCC 25 923), *Escherichia coli* (ATCC 25 922), human fibroblast (ATCC-CRL-4001, BJ-5ta) and keratinocyte (HaCat) cells were obtained from the American Type Culture Collection (ATCC LGC Standards, Spain). *Chromobacterium violaceum* (CECT 5999) was purchased from the Spanish Type Culture Collection (CECT, Spain).

2.2. Preparation and Characterization of Citronellal-Loaded Lauryl Gallate Nanoparticles (CLG_NPs)

Briefly, 0.02% (w/v) LG and 5% (v/v) citronellal were dissolved in ethanol. The solution was mixed with 1% (v/v) tween 80 in water in a 1:1 ratio and sonicated at 35% amplitude and 20 °C for 6 min in a VCX750 Sonics Vibra-Cell ultrasonic processor (Sonics and Materials Inc., USA). The sample was filtered by centrifugation (filter pore size 100 KDa) for 15 min at 1500 rpm, resuspended in Milli-Q water, and stored at 4 °C until use. The size of the CLG_NPs was determined by environmental electron microscopy (ESEM) in a Phenom Pro desktop scanning electron microscope (SEM) (Thermo-Fischer, USA). The NPs surface charge (ζ-potential) was measured with a Zetasizer Nano Z (Malvern Instruments, Netherlands). The amount of citronellal encapsulation in the CLG_NPs was determined by measuring the concentration of LG and citronellal before and after the synthesis using HPLC (Agilent/Series 1200), as previously described.[24] The antioxidant activity of the CLG_NPs was assessed by the DPPH free radical scavenging method.[17] Minimal inhibitory concentration (MIC) of the CLG_NPs against *S. aureus* (ATCC 25 923) and *E. coli* (ATTC 25 922) was determined following the Clinical and Laboratory Standards Institute recommendations.[25]

2.3. Quorum Sensing (QS) Inhibition Assay

The efficacy of the CLG_NPs for inhibiting biofilm formation was validated by assessing the NPs quorum sensing (QS) inhibition performance using two different approaches. Briefly, the

© 2025 The Author(s). Advanced Materials Interfaces published by Wiley-VCH GmbH

21967350, 2025, 13, Downloaded from https://advanced.onlinelibrary.wiley.com/doi/10.1002/admi.202401016 by Politecnico Di Torino Sist. Bibl Del Polit Di Torino, Wiley Online Library on [24/10/2025]. See the Terms and Conditions (https://onlinelibrary.wiley.com/terms-and-conditions) on Wiley Online Library for rules of use; OA articles are governed by the applicable Creative Commons License

inhibition of QS in Gram-negative bacteria was studied using *C. violaceum* like bacteria model, which produces violacein in the presence of AHL, a signal compound involved in cell-to-cell communication.[26] *C. violaceum* was incubated in LB broth at 27 °C and 180 rpm for 16 h. After incubation, the culture was mixed with LB soft agar supplemented with kanamycin (25 µM), and the suspension was adjusted to a final optical density at 600 nm (OD_{600}) of 0.01. Then, 5 mL of the mixture was poured into previously prepared LB agar plates to grow a bacterial lawn. The QS inhibition assay was performed by mixing 10 µM of the QS inducer AHL plus 100 µL of 5 mM PBS (pH 7.4) (control) or 100 µL of CLG_NPs diluted 1:1000 in 5 mM PBS (pH 7.4). Later, 10 µL of each reaction mixture was soaked on a sterile filter disk (5.5 mm diameter) and gently placed on the surface of LB agar plates pre-inoculated with *C. violaceum* and incubated for 16 h at 27 °C. The anti-QS activity of the CLG_NPs was confirmed by measuring the size of the violet halo around the disks and compared to the control condition (i.e., disk containing AHL without CLG_NPs addition). Finally, images of the plates were taken and analyzed using the software ImageJ.

Alternatively, to assess QS inhibition in a Gram-positive bacterial model, a genetically modified strain of methicillin-resistant *S. aureus* (USA300 LAC) that expresses green fluorescent protein (GFP) under a QS-dependent promoter was used.[27] This strain, $USA300_{agr\ IR\ P2\text{-}GFP}$, contains a *gfp* transcriptional fusion linked to the P2 promoter, which regulates the *agr* QS system. Briefly, overnight cultures of *S. aureus* ($USA300_{agr\ IR\ P2\text{-}GFP}$) were grown in tryptic soy broth (TSB) at 37 °C with shaking and diluted to an OD_{600} = 0.01 in LB. Then, 50 µL of CLG _NPs, bulk LG, citronellal, or LG_NPs were incubated with 50 µL of the bacterial culture for 12 h at 37 °C with shaking. After incubation, the expression driven by the QS-dependent promoter was measured fluorometrically at λ_{ex}485/ λ_{em}535 nm at room temperature using a microplate reader (Infinite M200, TECAN, Austria).

2.4. Polydimethylsiloxane Functionalization

Laminar pieces (1 × 1 cm) of PDMS, from which the urinary catheters were produced, were washed sequentially with 0.1% (w/v) SDS solution, deionized water, and 96% ethanol. Then, the PDMS samples were incubated in a buffered solution (pH = 5) consisting of CS 0.5% (w/v) and CLG_NPs in a 2:1 ratio. The solution was sonicated for 30 min at 20 °C in a VCX750 Sonics Vibra-Cell ultrasonic processor (Sonics and Materials Inc., USA) set at 50% amplitude.

2.5. Coating Characterization

2.5.1. Microscopy Analysis

The surface topography of pristine PDMS samples and those coated with CS, CLG_NPs, or CS/CLG_NPs was assessed by AFM in a Multimode Nanoscope 8 system (Bruker, USA) under ambient conditions. Coated and uncoated PDMS pieces (1 × 1 cm) were fixed to a poly(tetrafluoroethylene) (PTFE) surface, and subsequently adhered onto a metallic AFM disc. The Nanoscope Analysis v1.5 software was used for images processing. Additionally, the coatings on the surface of the PDMS samples were visualized using confocal scanning laser microscopy (CSLM, Zeiss LSM 800 system, Carl Zeiss, Germany) by labelling the CLG_NPs with Nile red fluorophore[28] and CS with green FITC fluorophore.[29]

2.5.2. Water Contact Angle (WCA)

The WCA of pristine and coated PDMS samples was quantified using a DSA25 Drop Shape Analyzer (Krüss GmbH, Germany) and the Krüss Advanced software (v1.13.0.21301). The sessile drop method was used to measure the contact angle as previously described.[30] The stability of the coating on the PDMS surface was evaluated by comparing the difference in the contact angle between freshly coated samples and those incubated for 7 days (37 °C, 100 rpm) in deionized water after coating.[9]

2.5.3. Citronellal Release Kinetics

The release of citronellal from CLG_NPs and CS/CLG_NPs coated PMDS was assessed by HPLC at different pHs. Briefly, coated PDMS samples (1 × 1 cm) were immersed in 2.0 mL sterile PBS adjusted to pH 6 – 8 (pH values within the normal human urine range) and incubated at 37 °C in a water bath with shaking (100 rpm). Every 24 h the samples were removed and immersed in fresh PBS solution. The release of citronellal was assessed using an Agilent Technologies 1200 Series HPLC system (Agilent Technologies, USA) equipped with a Microsorb-MV C-18 reversed-phase column (150 × 4.6 mm^2; particle size, 5 µm; Agilent Technologies, USA). A gradient elution was used with H_2O: acetonitrile (1:5) as the mobile phase at a flow rate of 0.5 mL min^{-1}. A Citronellal signal was detected using a diode array detector set at 285 nm. For building the calibration curve, standard solutions of citronellal (0.02, 0.03, 0.06, 0.13, 0.25, 0.50, 1.00, and 2.00 mg L^{-1}) were employed. The calibration process displayed reproducible linear relationship ($R^2 > 0.995$).

2.6. Radical Scavenging Activity of the Coating

The antioxidant activity of pristine and coated PDMS samples (1 × 1 cm) was assessed by the DPPH free radical scavenging method.[31] Samples were immersed in a solution containing 60 µM DPPH. After 1 h incubation in the dark, the absorbance of the samples was measured at 517 nm. A solution of ascorbic acid (1.0 mg mL^{-1}) was used as the positive control for the assay.

2.7. Antimicrobial and Antibiofilm Properties

2.7.1. Antimicrobial Activity Against Planktonic Bacteria

The antimicrobial activity of pristine and coated PDMS samples was assessed following the ASTM-E2149-20 method. Single colonies of *E. coli* (ATCC 25 922) and *S. aureus* (ATCC 25 923) were cultured overnight in 5 mL sterile Mueller-Hinton broth at 37 °C and 230 rpm. The cultures were then diluted with sterile PBS (pH = 7.4) to an OD_{600} = 0.28. Subsequently, the solution was further diluted to 1:1000 in sterile PBS (pH = 7.4), and

© 2025 The Author(s). Advanced Materials Interfaces published by Wiley-VCH GmbH

21967350, 2025, 13, Downloaded from https://advanced.onlinelibrary.wiley.com/doi/10.1002/admi.202401016 by Politecnico Di Torino Sist. Bibl Del Polit Di Torino, Wiley Online Library on [24/10/2025]. See the Terms and Conditions (https://onlinelibrary.wiley.com/terms-and-conditions) on Wiley Online Library for rules of use; OA articles are governed by the applicable Creative Commons License

the PDMS samples (1 × 1 cm) were incubated with 1.5 mL of the diluted bacterial suspension. After 24-h incubation (37 °C, 230 rpm) the surviving bacteria were quantified by colony counting on Coliform ChromoSelect or Baird-Parker agar for *E. coli* and *S. aureus* growth, respectively.

2.7.2. Biofilm-Forming Assay

The efficacy of the developed coating for inhibiting biofilm formation was evaluated using the crystal violet staining method.[32] Briefly, pristine and CS-, CLG_NPs- and CS/CLG_NPs- coated PDMS samples (1 × 1 cm) were incubated in a 24-well microplate with 1.5 mL (OD_{600} = 0.01) of a bacterial suspension (*E. coli* or *S. aureus*) prepared in TSB. The microplate was incubated for 24 h at 37 °C under static conditions, allowing bacteria to colonize the PDMS surface and form biofilm. Following incubation, the non-adhered bacterial cells were removed by washing the samples with sterile PBS (pH 7.4). Later, the bacterial biofilms attached to the surface of the PDMS pieces were dried at 60 °C for 60 min, and stained with 1 mL of 0.1% (w/v) crystal violet solution for another 15 min. Subsequently, the PDMS pieces were placed with 1 mL of 30% acetic acid (v/v) to solubilize the crystal violet dye on the samples. Finally, 200 µL of this solution was transferred to a new 96-well plate and the absorbance was measured at 595 nm in a TECAN Infinite M200 microplate reader (TECAN, Austria). The assay was performed in triplicates (n = 3).

2.7.3. Bacterial Viability Quantification in Biofilms

Pristine, CS-, CLG_NPs- and CS/CLG_NPs- coated PDMS samples (1 × 1 cm) were incubated in a 24-well microplate for 24 h at 37 °C under static conditions with 1.0 mL of *E. coli* or *S. aureus* suspension (OD_{600} = 0.01) prepared in TSB. After incubation, the samples were washed 3 times with 1 mL of sterile PBS (pH = 7.4) to remove the non-attached cells and transferred into 15 mL test tubes containing 2 mL of sterile PBS (pH = 7.4). Later, the tubes were vortexed for 3 min and placed in an ultrasonic bath for 20 min for detaching bacteria. Finally, the number of viable *E. coli* and *S. aureus* was determined by plating 10 µL of the supernatant (diluted from 1 to 10^{-6}) on Coliform CromoSelect or Baird-Parker agar plates, respectively. Additionally, a qualitative evaluation of the viability of the biofilm attached to the surface of pristine and coated PDMS samples was performed using the Live/Dead BacLight kit following the supplier´s recommendations. Confocal fluorescence micrographs were taken with an inverted laser scanning microscope at λ_{ex}480/ λ_{em}500 nm for Syto 9 detection (green-fluorescent probe for live bacteria staining) and at λ_{ex}490/λ_{em}635 nm for propidium iodide detection (red-fluorescent probe for dead bacteria staining).

2.7.4. In Vitro Dynamic Model of Catheterized Bladder for Biofilm Testing

An in vitro model that simulates a catheterized human bladder environment was used to assess the efficacy of the CS/CLG_NPs coating for inhibiting biofilm formation on catheters under dynamic conditions.[30] Both pristine and CS/CLG_NPs-coated silicone Foley catheters were inserted into the system, and the catheters' balloons were filled with 5 mL of 100 mM PBS (pH = 7.4). Subsequently, the artificial bladder was filled up to the catheter's eye with sterile artificial urine (adjusted to pH = 6.8) prepared following the UNE EN1616 (Sterile Urethral Catheters for Single Use) guidelines and supplemented with 1 mg mL^{-1} TSB, Gram-negative *E. coli*, and Gram-positive *S. aureus* (OD_{600} = 0.005 for each bacteria culture) (**Figure 1**). The system was maintained at 37 °C for 7 days with a continuous supply of fresh sterile artificial urine at a flow rate of 1 mL min^{-1}. After this period, the catheter was removed and the bacterial biomass (i.e., biofilm) formed on the catheter tip and the balloon was assessed by crystal violet staining as described in Section 2.6.2.

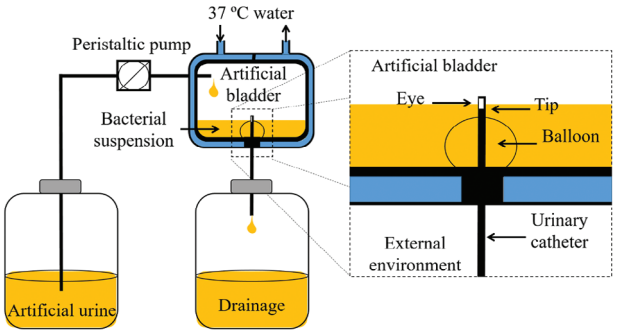

Figure 1. Scheme of the experimental setup simulating a human bladder used for testing the antibiofilm performance of coated catheters.

2.8. Assessment of Coating Biocompatibility and Antioxidant Activity

Fibroblasts (BJ-5ta) and keratinocytes (HaCat) were previously seeded at a density of 4.5 × 10^4 cells per well on a sterile 24–well tissue culture polystyrene plate. For the cytotoxicity assessment, pristine and CS/LG_NPs-coated PDMS pieces (1 × 1 cm) were placed in direct contact with the cells. Then, 0.75 mL of complete growth medium (DMEM) was added to each well and the plate was incubated at 37 °C in a humidified atmosphere of 5% CO_2 for 24 h. Later, the cells were examined for signs of toxicity using the Alamar Blue assay kit, following the supplier's recommendation. Cells subjected to the same conditions but without the presence of PDMS were used as controls. Furthermore, the viability of fibroblasts and keratinocytes was assessed using the Live/Dead Viability/Cytotoxicity kit, according to the manufacturer's instructions.

2.9. Statistical Analysis

All reported data were presented as the mean value ± standard deviation (S.D.). Multiple comparisons were performed using the GraphPad Prism Software (version 5.04). One-way analysis of variance (ANOVA) followed by either a post-hoc Tukey's test or the unpaired two-tailed Student's t-test method was applied. Statistical significance was defined as p-values less than 0.05 (*), 0.01 (**), or 0.001 (***), denoting different levels of significance in the statistical analysis.

© 2025 The Author(s). Advanced Materials Interfaces published by Wiley-VCH GmbH

21967350, 2025, 13, Downloaded from https://advanced.onlinelibrary.wiley.com/doi/10.1002/admi.202401016 by Politecnico Di Torino Sist. Bibl Del Polit Di Torino, Wiley Online Library on [24/10/2025]. See the Terms and Conditions (https://onlinelibrary.wiley.com/terms-and-conditions) on Wiley Online Library for rules of use; OA articles are governed by the applicable Creative Commons License

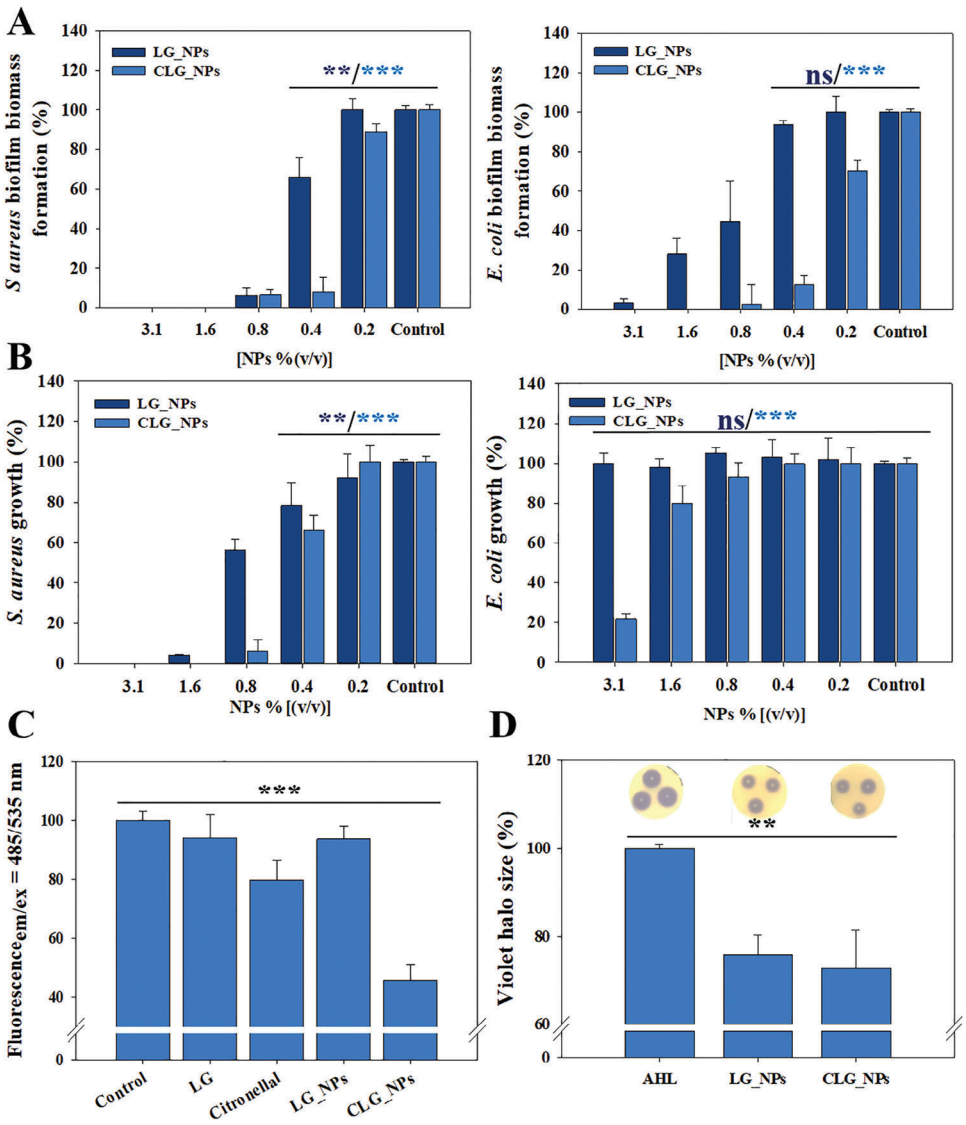

Figure 2. A) Antibiofilm and B) antimicrobial activity of LG_NPs and CLG_NPs against *S. aureus* and *E. coli*. Quorum quenching activity of LG_NPs and CLG_NPs against C) *S. aureus* USA300$_{agr\ IR\ P2\text{-}GFP}$ and D) *C. violaceum*. Data are presented as the mean value ± S.D. ($n = 3$).

3. Results and Discussion

3.1. Synthesis and Characterization of CLG_NPs

The US-assisted emulsification method used in this work for the synthesis of CLG_NPs (Figure S1, Supporting Information) is a simple approach for preparing stable core-shell NPs, where the hydrophobic aliphatic tails of LG are oriented inward, while the phenolic heads face outward, forming a protective shell around the citronellal core.[33] The sonication conditions (e.g., temperature, time, and amplitude) employed during CLG_NPs synthesis ensured the production of particles with a homogeneous size of ≈700 nm as confirmed by SEM imaging (Figure S2, Supporting Information), and ζ-potential of −35 ± 1 mV, indicating good colloidal stability. In contrast, the control LG_NPs, synthesized in the absence of citronellal, showed ζ-potential of −25 ± 1 mV, but the resulting suspension was unstable and precipitated after 24 h storage (Figure S3, Supporting Information). We believe this difference in the stability is due to the hydrophobic interactions between LG alkyl chain and citronellal, which facilitate the formation of the NPs core, while the hydrophilic phenolic shell stabilizes the NPs in the water suspension.[34] Additionally, 95% of LG were successfully nanoformulated during the synthesis of CLG_NPs, compared to only 75% in the case of LG_NPs. This suggests that the presence of citronellal improves the efficiency of LG-based NPs synthesis (serving as both encapsulating and structural agents in the coating) and enhances their stability, possibly due to hydrophobic interactions with the aliphatic tails of LG. Moreover, a 40% citronellal encapsulation in CLG_NPs was achieved during synthesis, as determined by HPLC.

Both LG_NPs and CLG_NPs inhibited the biofilm formation of *S. aureus* and *E. coli* (**Figure** 2A,B), two of the most common pathogens found in biofilm-associated CAUTIs.[35] These results align with our expectations, given the known antimicrobial

 © 2025 The Author(s). Advanced Materials Interfaces published by Wiley-VCH GmbH

21967350, 2025, 13, Downloaded from https://advanced.onlinelibrary.wiley.com/doi/10.1002/admi.202401016 by Politecnico Di Torino Sist. Bibl Del Polit Di Torino, Wiley Online Library on [24/10/2025]. See the Terms and Conditions (https://onlinelibrary.wiley.com/terms-and-conditions) on Wiley Online Library for rules of use; OA articles are governed by the applicable Creative Commons License

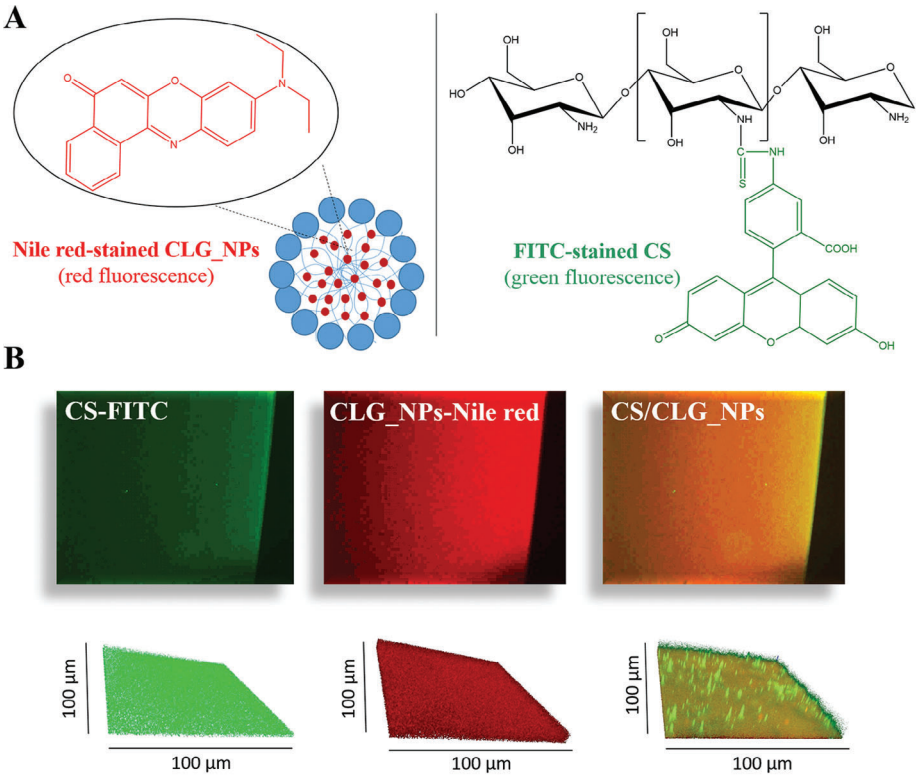

Figure 3. A) Schematic representation of Nile red-stained CLG_NPs and FITC-stained CS. B) Confocal micrographs of silicone (PDMS) surface after the sonochemical deposition of CS (green), CLG_NPs (red) or the hybrid CS/CLG_NPs coating (orange).

properties of both LG and citronellal.[19,36] Nevertheless, the inclusion of citronellal in LG_NPs (i.e., CLG_NPs), not only enhanced their antimicrobial and antibiofilm activities at lower concentrations, but also provided an additional mechanism for inhibiting biofilm formation by interfering with bacterial quorum sensing (QS) process (**Figure** 2C,D). These results agreed with previous reports demonstrating alkyl gallate potential for affecting biofilm formation and QS in other bacterial species of clinical relevance, e.g., *Pseudomonas aeruginosa*.[37,38] Notably, our results are the first to describe anti-QS activity of citronellal, in particular, against both Gram-positive and Gram-negative bacteria, adding to the growing knowledge on the QS-regulation and antibiofilm effect of EOs.[13,14]

3.2. Physicochemical Characterization of the Nanocomposite Coatings

The CLG_NPs and CS were co-deposited onto PDMS catheter material using high-intensity US process. This waterborne method avoids the use of harsh reaction conditions and toxic compounds to efficiently coat substrates with various surface chemistries,[9] aligning with sustainability goals in industrial manufacturing. During the sonochemical process, both CLG_NPs and CS are projected toward the silicone surface upon the collapse of cavitation bubbles, building the coating, without the need for silicone surface pre-activation.[39] The adherence of the coating to the inert silicone material is primarily attributed to the interaction and self-assembly of phenolic shell NPs with amino and hydroxyl groups of chitosan, leading to adherence and insolubility of the coating. This interaction mimics the strong surface adhesion mechanisms of the mussel-inspired chemistry, a simple and efficient strategy previously used in our group for the generation of durable NP-coatings on silicone material.[9] Additionally, under the US field, the generated high-energy microjets drive the coating components (i.e., nanoparticles, chitosan) onto the silicone surface, where they adhered firmly through physicochemical interactions.

The hybrid CS/CLG_NPs coating on the surface of silicone samples was visualized by confocal microscopy using two distinctive fluorescent probes: Nile red encapsulation (red fluorescence) for labelling CLG_NPs and FITC-grafting (green fluorescence) for CS (**Figure** 3A). The PDMS sample coated with CS/CLG_NPs exhibited an orange fluorescence, characteristic of the combined fluorescence signals from the green-labelled CS and the red-labelled CLG_NPs (red), confirming the successful deposition of both components on the silicone surface.

Additionally, the surface morphology of silicone samples coated with CS, CLG_NPs, and CS/CLG_NPs was investigated by AFM (**Figure** 4). The presence of CS alone did not exhibit a significant difference compared to the pristine PDMS sample (Figure 4A,B). However, the surface heterogeneity of both CLG_NPs- and CS/CLG_NPs-coated material notably increased compared to the pristine silicone. The average roughness value (R_A) and the root-mean-square roughness (R_Q) increased from 6.2 ± 2.8 µm and 8.8 ± 4.8 µm to 12.3 ± 7.6 µm and 17.8

© 2025 The Author(s). Advanced Materials Interfaces published by Wiley-VCH GmbH

21967350, 2025, 13, Downloaded from https://advanced.onlinelibrary.wiley.com/doi/10.1002/admi.202401016 by Politecnico Di Torino Sist. Bibl Del Polit Di Torino, Wiley Online Library on [24/10/2025]. See the Terms and Conditions (https://onlinelibrary.wiley.com/terms-and-conditions) on Wiley Online Library for rules of use; OA articles are governed by the applicable Creative Commons License

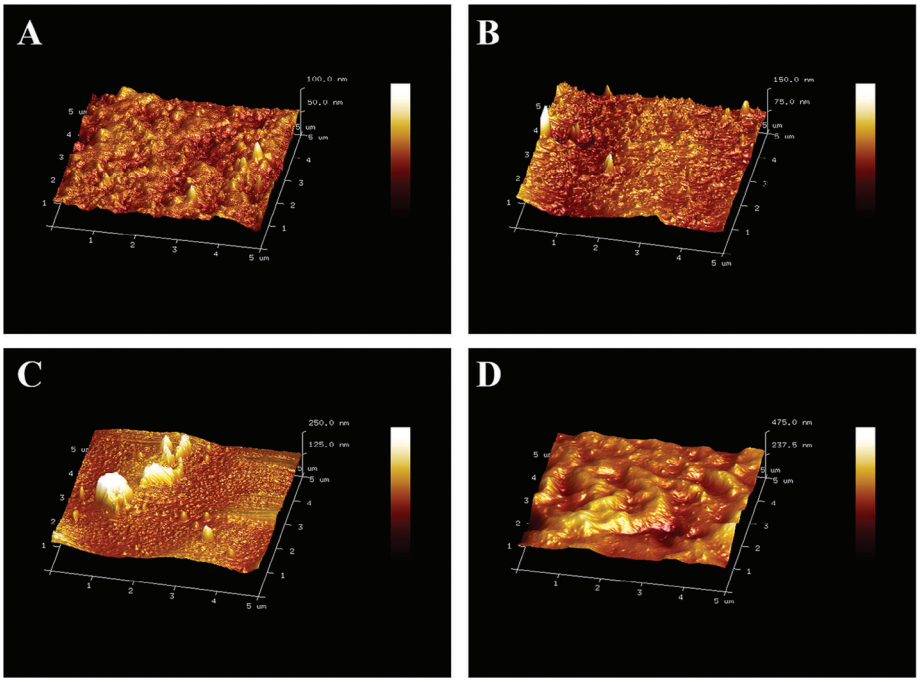

Figure 4. AFM surface micrographs of A) pristine silicone and silicone after the sonochemical deposition of B) CS, C) CLG_NPs, and D) the hybrid CS/CLG_NPs composite.

± 10.7 µm for the CLG_NPs, and to 18.0 and 18.0 ± 4.9 µm and 23.5 ± 6.9 µm for the hybrid CS/CLG_NPs, proving the coatings were successfully built-up on the PDMS surface. Despite this, the nanometric scale of the surface roughness of the coating ensures that it would not cause discomfort in the catheterized patient.

In addition, coating deposition was further confirmed by the reduction of PDMS hydrophobicity (**Figure 5A**) due to the inherent hydrophilic nature of CS (containing amino groups) and CLG_NPs (containing phenolic groups). This increase in surface hydrophilicity provides an additional advantage, as it would facilitate the catheterization procedure serving as a lubricant. The data in Figure 5A showed that the hybrid coating remained on the PDMS sample after a 7-day incubation in water, as no significant changes were detected in the WCA values between T0 and T7. The stability of the CS/CLG_NPs coating is likely attributed to multiple interactions, including electrostatic forces between CS and CLG_NPs.[40,41] Hydrophobic interactions, supported by dispersive forces (e.g., van der Waals), between the LG chains and the hydrophobic regions of CS (acetyl groups), along with hydrogen bonding between LG hydroxyl groups and CS polar groups, further provide coating stabilization. These interactions can result in denser and more durable monolayers,[42] which is critical for preventing catheter surface colonization, particularly when using bio-based composite materials with antimicrobial properties.[43]

Finally, both CLG_NPs and CS/CLG_NPs demonstrated antioxidant capacity due to the presence of citronellal and gallate in their composition (Figure 5B). Reactive oxygen species (ROS) scavenging would preserve the urinary tract from biofilm-associated oxidative stress. For instance, tissue damage caused by uropathogenic *E. coli* is associated with increased production of ROS.[44,45] During infections like CAUTIs, immune responses also generate ROS to combat pathogens. Excess ROS can inadvertently harm the bladder's epithelial cells and impair their barrier function.[46] Therefore, antioxidant activity represents a novel feature in catheter coatings, whereas the primary focus has traditionally been on antimicrobial and antibiofilm activities.

3.3. Citronellal Release Kinetics

The amount of citronellal released from PDMS samples coated with CLG_NPs or CS/CLG_NPs was quantified using HPLC. The pH of the medium in contact with the coated material varied from 6 to 8 (normal pH values of urine). The released EO from the samples coated with the hybrid CS/CLG_NPs coating was less than 30% in all cases.

In general, the presence of CS in the hybrid coating reduced the release of citronellal compared to the CLG_NPs-coated PDMS samples at all tested pHs (**Figure 6**). This can be attributed to multiple non-covalent interactions, e.g., electrostatic, dispersive, hydrophobic, and hydrogen bonding between CS and the CLG_NPs and citronellal alone, which hinder the release of EO. Reduced porosity of the coating as a result of CS molecular self-assembly[15] may further retard the EO release. These findings are also supported by the higher stability of the hybrid coating after 7 days of incubation (Figure 5).[47,48]

Notably, at pH 6, the release of citronellal from CLG_NPs-coated PDMS samples was significantly higher compared to the citronellal loss from the silicone material coated with CS/CLG_NPs. The pH of the medium plays a crucial role in the interaction of CS with charged molecules due to partial protonation or deprotonation of its amine groups. The NH_2 of CS (pKa ~6.5) can be partially protonated in weakly-acidic media

 © 2025 The Author(s). Advanced Materials Interfaces published by Wiley-VCH GmbH

21967350, 2025, 13, Downloaded from https://advanced.onlinelibrary.wiley.com/doi/10.1002/admi.202401016 by Politecnico Di Torino Sist. Bibl Del Polit Di Torino, Wiley Online Library on [24/10/2025]. See the Terms and Conditions (https://onlinelibrary.wiley.com/terms-and-conditions) on Wiley Online Library for rules of use; OA articles are governed by the applicable Creative Commons License

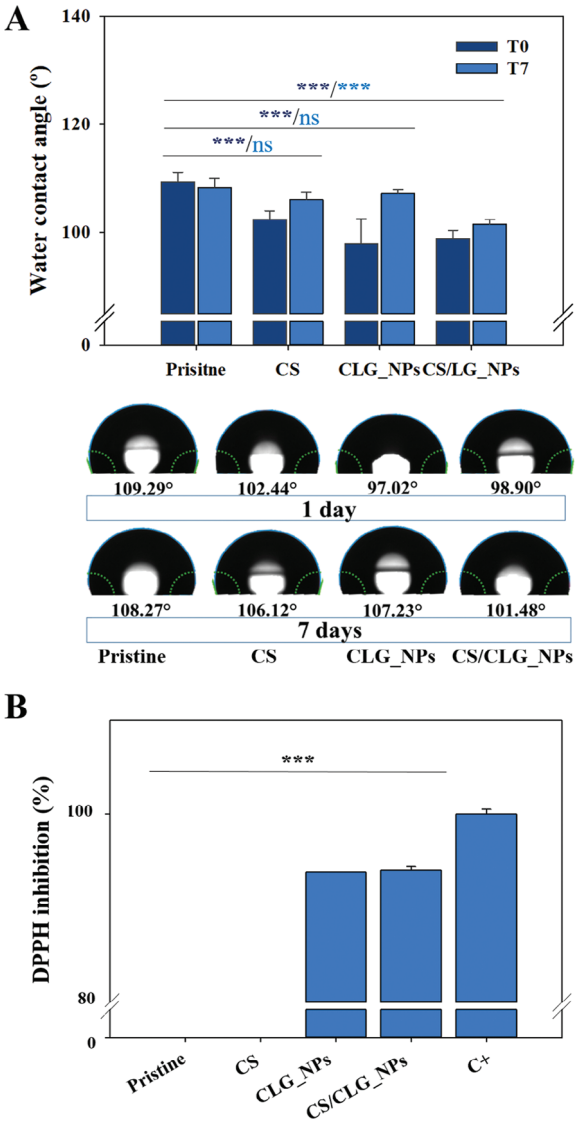

Figure 5. A) The water contact angle of coated silicone samples. The dark blue bars represent the values obtained immediately after the coating deposition, while the light blue ones report data obtained after 7-day incubation in water (at 25 °C, with 100 rpm shaking). Data are presented as mean value ± S.D. ($n = 10$). B) Antioxidant activity of uncoated (pristine) and CS-, CLG_NPs- and CS/CLG_NPs- coated PDMS samples. Ascorbic acid (1.0 mg mL^{-1}) was used as the positive control (C+). Data are presented as the mean value ± S.D. ($n = 3$).

causing an increase in the electrostatic forces that attract anionic molecules. Therefore, a stronger interaction between the anionic CLG_NPs and CS could be expected at pH 6, thus limiting citronellal release. The opposite can be observed at pH values over 6.5 due to NH_2 group deprotonation. In fact, at neutral-basic pHs (7 – 8) citronellal release from the hybrid coating was higher than at pH 6, and comparable to the values obtained for the CLG_NPs-coated material at pH 8. This result is interesting since consistently alkaline urine with pH > 7 can be supportive of urinary tract infections associated with urease-producing organisms such as *P. aeruginosa*, *S. aureus*, and *Proteus* spp.[49] The

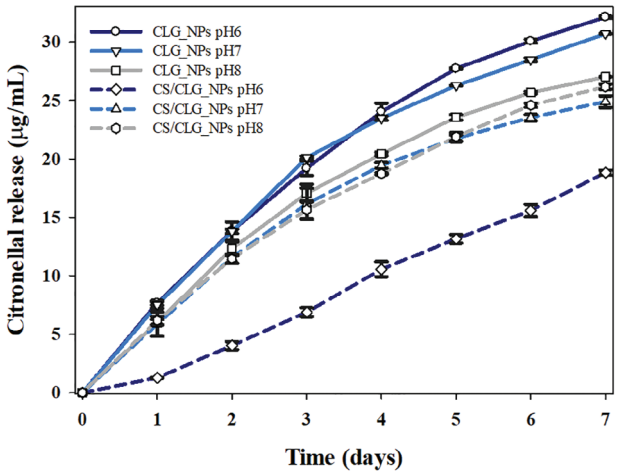

Figure 6. Kinetics of citronellal release from CLG_NP and CS/CLG_NPs-coated PDMS samples at different pHs. Data are presented as the mean value ± S.D. ($n = 3$).

hybrid coating releases more antimicrobial citronellal at neutral-basic pHs in response to potential bacteriuria.

At acidic pHs lower than pH 6, a higher protonation of the $-NH_2$ groups of CS occurs, increasing its solubility and consequently instability of the hybrid coating. In line with the pH values commonly observed in human urine from patients with urinary tract infections, our study focused on the pH range from 6 to 8, considering that different uropathogenic bacteria can influence urine acidity through their metabolism when interacting with the host.[49]

3.4. Antimicrobial and Antibiofilm Properties of the Nanocomposite Coatings

The viability of *E. coli* and *S. aureus* decreased by 2–3 logs for CLG_NPs- and CS/CLG_NPs-coated PDMS samples after 24 h incubation in a PBS-buffered solution at pH 7.4 (**Figure 7**). These results correlate with the increased release of antimicrobial citronellal from the coating at pH 7–8 (Figure 6). Despite the

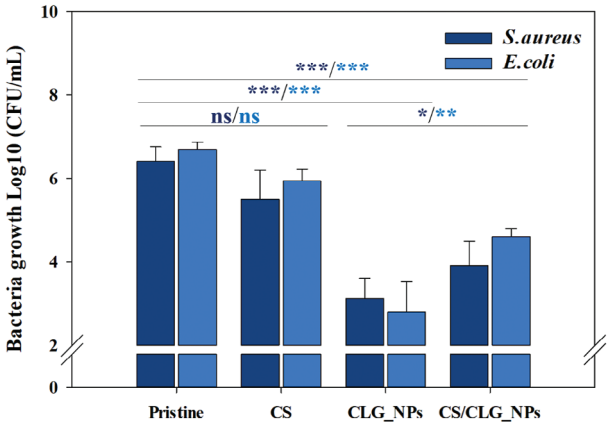

Figure 7. Antibacterial activity against planktonic bacteria of coated silicone samples. Data are presented as the mean value ± S.D. ($n = 3$).

© 2025 The Author(s). Advanced Materials Interfaces published by Wiley-VCH GmbH

21967350, 2025, 13, Downloaded from https://advanced.onlinelibrary.wiley.com/doi/10.1002/admi.202401016 by Politecnico Di Torino Sist. Bibl Del Polit Di Torino, Wiley Online Library on [24/10/2025]. See the Terms and Conditions (https://onlinelibrary.wiley.com/terms-and-conditions) on Wiley Online Library for rules of use; OA articles are governed by the applicable Creative Commons License

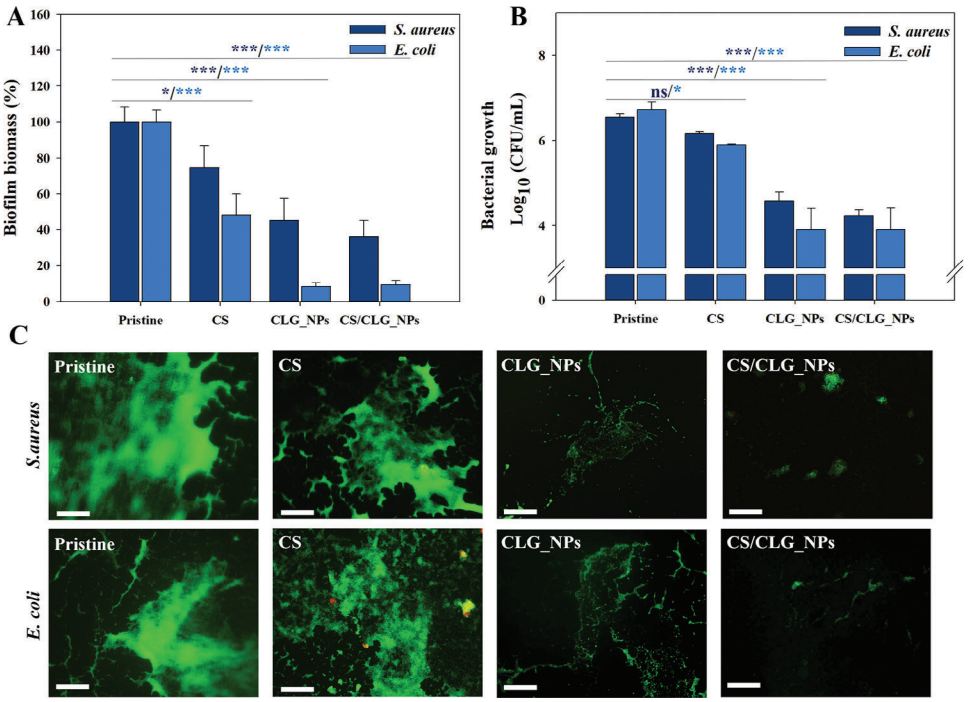

Figure 8. A) Biofilm inhibition and B) Biofilm viability assessment on coated and uncoated silicone samples in static conditions after 24 h. C) Fluorescence microscopy images of live (green) and dead (red) bacteria on coated and uncoated silicone samples. Green and red fluorescence images are overlapped. Scale bar 100 µm.

intrinsic antimicrobial properties reported for CS, no significant reduction in the viability of planktonic bacteria was observed for the CS-coated silicone samples compared to the uncoated material.

CS-coated PDMS showed, however, a significant reduction in the amount of biofilm formed on the material compared to the pristine PDMS (**Figure 8**). Coatings containing CLG_NPs proved to be more efficient in preventing biofilm formation as supported by the higher reduction of *S. aureus* and *E. coli* biomass deposited on CLG_NPs- and CS/CLG_NPs-coated materials (Figure 8A), corroborating the results for the antibacterial activity of the coating against planktonic bacteria as well (Figure 7). Moreover, the viability of the surface-attached microbial cells was reduced by 2 logs on the silicone samples coated with CLG_NPs and the hybrid CS/CLG_NPs composite (Figure 8B). Fluorescence microscopy observations further demonstrated higher biofilm formation on pristine and CS-coated samples compared to CLG_NPs- and CS/CLG_NPs-coated PDMS (Figure 8C). The highest antibiofilm activity was achieved for the hybrid coating, suggesting a synergistic effect of CS and CLG_NPs. The absence of red fluorescence in Figure 8C indicates that the predominant mechanism of biofilm inhibition is preventing bacterial adhesion to the coated material and/or reducing the number of viable planktonic cells (Figure 7), rather than affecting sessile bacteria on the silicone surface.

The antibiofilm performance of the nanocomposite coating was also assessed in an in vitro dynamic model simulating the urinary tract environment. Pristine and CS/CLG_NPs coated catheters were introduced into an artificial bladder inoculated with bacteria and supplied with sterile artificial urine (pH 6.8) at a flow rate of 1 mL min^{-1}. These conditions replicate the flow in urinary catheters connected to drainage bags, mimicking the daily urine production by an adult (0.8–2.0 L).[10] After 7 days urine recirculation, the catheters were collected, sectioned, and stained with crystal violet to assess the amount of biofilm deposited on the catheter's surface. The hybrid CS/CLG_NPs coating substantially prevented biofilm formation (**Figure 9**) indicating durable antibiofilm performance under close-to-real application conditions. Therefore, the durability of the coating

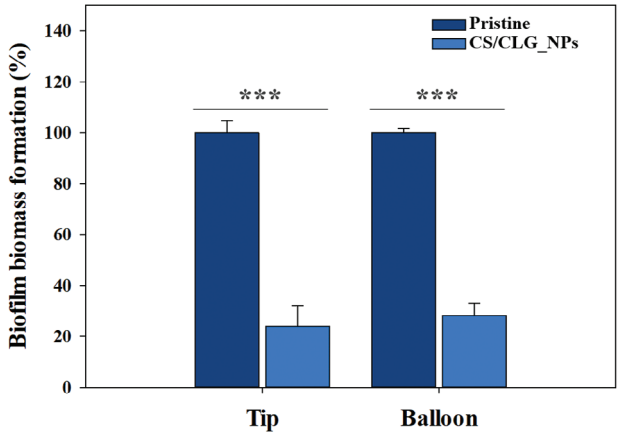

Figure 9. Biofilm biomass quantification by crystal violet staining on pristine and CS/CLG_NPs coated catheter sections (tip and balloon) after 7 days of infected urine recirculation in an artificial bladder. Data are presented as the mean value ± S.D. ($n = 3$).

© 2025 The Author(s). Advanced Materials Interfaces published by Wiley-VCH GmbH

21967350, 2025, 13, Downloaded from https://advanced.onlinelibrary.wiley.com/doi/10.1002/admi.202401016 by Politecnico Di Torino Sist. Bibl Del Polit Di Torino, Wiley Online Library on [24/10/2025]. See the Terms and Conditions (https://onlinelibrary.wiley.com/terms-and-conditions) on Wiley Online Library for rules of use; OA articles are governed by the applicable Creative Commons License

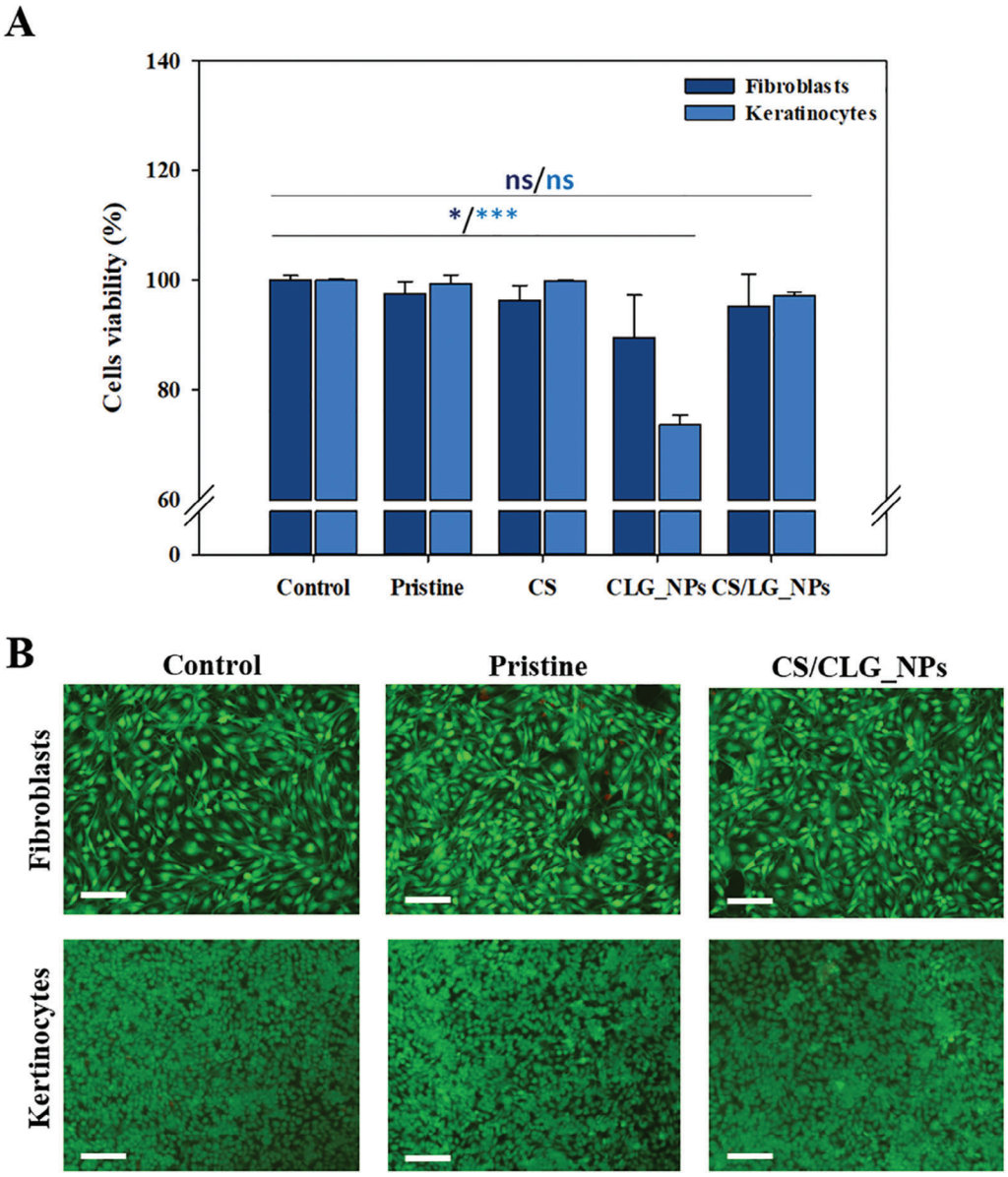

Figure 10. Viability of fibroblast (BJ-5ta) and keratinocyte (HaCat) cell line after 24 h exposure to uncoated (pristine) or coated silicone samples. A) Cell viability was assessed by the Alamar Blue colorimetric test. Data are presented as the mean value ± S.D. ($n = 3$). B) Representative images of Live/Dead staining of fibroblasts and keratinocyte cells after being co-cultured with pristine or CS/CLG_NPs-coated PDMS samples. The green and red fluorescence images are overlapped. Scale bars 100 µm.

(Figure 5), combined with its ability to maintain antimicrobial/antibiofilm activity under continuous urine flow, represents a substantial advancement in the design of catheter coatings since most studies report antimicrobial efficacy for shorter periods (e.g., 24–72 h) or under static conditions.

3.5. Coatings Biocompatibility

Biocompatibility is a critical property for the validation of indwelling medical devices. Testing fibroblast and keratinocyte viability is crucial when assessing catheter coating biocompatibility, as these cell types represent different aspects of the tissue response. Fibroblasts reflect the subcutaneous tissue interaction, while keratinocytes help evaluate potential inflammatory or cytotoxic effects from prolonged catheter surface contact. No significant alteration of human fibroblasts and keratinocyte viability was detected after 24 h of direct contact with the hybrid CS/CLG_NPs coating, confirming its biocompatibility (**Figure 10**A). Moreover, the coating did not induce any morphological changes in the tested human cells suggesting its suitability for biomedical application (Figure 10B). On the other hand, CLG_NPs-coated PDMS samples slightly affected cell viability, probably due to the higher amount of citronellal released

© 2025 The Author(s). Advanced Materials Interfaces published by Wiley-VCH GmbH

21967350, 2025, 13, Downloaded from https://advanced.onlinelibrary.wiley.com/doi/10.1002/admi.202401016 by Politecnico Di Torino Sist. Bibl Del Polit Di Torino, Wiley Online Library on [24/10/2025]. See the Terms and Conditions (https://onlinelibrary.wiley.com/terms-and-conditions) on Wiley Online Library for rules of use; OA articles are governed by the applicable Creative Commons License

from those samples (Figure 6), which indicates the importance of coating stability for minimizing cytotoxic effects. These findings demonstrate that the hybrid CS/CLG_NPs coating is safe, with durable functionality, and hence suitable for clinical use.

4. Conclusion

In this study, we developed a bio-based nanocomposite coating on urinary catheters using a fast and simple waterborne sonochemical process. CLG_NPs in the coating served both as structural elements and as antimicrobial, antibiofilm, and antioxidant agents. Adhesive interactions between CS and CLG_NPs provided coating stability, durability, and controlled, pH-dependent citronellal release, without inducing cytotoxicity to human cells. In vitro tests demonstrated the coating's ability to prevent biofilm formation by inhibiting bacterial QS, while its antioxidant properties could mitigate the oxidative stress from both inflammation and bacterial activity in the urinary tract. The durable antimicrobial/antibiofilm performance of the coated catheters was validated in a simulated bladder environment, maintaining efficacy for at least one week of catheterization. The hybrid CS/CLG_NPs coating simultaneously addresses several early-stage pathogenic factors associated with CAUTIs, demonstrating the potential for preventing microbial adherence, colonization, and subsequent infection. Finally, the findings reported in this work contribute to the understanding of the efficacy, safety, and potential for clinical use of essential oils in catheter coatings.

Supporting Information

Supporting Information is available from the Wiley Online Library or from the author.

Acknowledgements

The authors acknowledge the grant PCI2024-153444 (SMARTGEL – Smart nanogels of bio-based antimicrobials to prevent urinary tract infections by disrupting inter- and intra-species communication of pathogens), funded by Agencia Estatal de Investigación (Ministerio de Ciencia e Innovación, España), under the European Union M-ERA.NET initiative. T.T. acknowledges the ICREA Academia award.

Conflict Of Interest

The authors declare no conflict of interest.

Data Availability Statement

The data that support the findings of this study are available from the corresponding author upon reasonable request.

Keywords

antimicrobial and antibiofilm coating, catheter-associated urinary tract infections, chitosan, citronellal, lauryl gallate, nanoparticles, sonochemistry

Received: December 20, 2024
Revised: January 27, 2025
Published online: March 13, 2025

[1] N. Sabir, A. Ikram, G. Zaman, L. Satti, A. Gardezi, A. Ahmed, P. Ahmed, *Am. J. Infect. Control* **2017**, *45*, 1101.
[2] A. Mazzariol, A. Bazaj, G. Cornaglia, *J. Chemother.* **2017**, *29*, 2.
[3] E. Y. Trizna, M. N. Yarullina, D. R. Baidamshina, A. V. Mironova, F. S. Akhatova, E. V. Rozhina, R. F. Fakhrullin, A. M. Khabibrakhmanova, A. R. Kurbangalieva, M. I. Bogachev, A. R. Kayumov, *Sci. Rep.* **2020**, *10*, 14849.
[4] C. Michaelis, E. Grohmann, *Antibiotics* **2023**, *12*, 328.
[5] M. J. Andersen, A. L. Flores-Mireles, *Coatings* **2020**, *10*, 23.
[6] S. Rajaramon, K. Shanmugam, R. Dandela, A. P. Solomon, *Front. Cell. Infect. Microbiol.* **2023**, *13*, 1134433.
[7] F. Gomollón-Bel, *Chem. Int.* **2021**, *43*, 13.
[8] A. Ivanova, K. Ivanova, T. Tzanov, *Nanomaterials* **2021**, *11*, 3143.
[9] A. Puertas-segura, K. Ivanova, A. Ivanova, I. Ivanov, K. Todorova, P. Dimitrov, G. Ciardelli, T. Tzanov, *ACS Appl. Mater. Interfaces* **2024**, *16*, 34656.
[10] A. Ivanova, K. Ivanova, I. Perelshtein, A. Gedanken, K. Todorova, R. Milcheva, P. Dimitrov, T. Popova, T. Tzanov, *Mater. Sci. Eng. C* **2021**, *131*, 112518.
[11] S. Malic, R. P. C. Jordan, M. G. J. Waters, D. J. Stickler, D. W. Williams, *Antimicrob. Agents Chemother.* **2014**, *58*, 1192.
[12] F. Maggio, C. Rossi, A. Serio, C. Chaves-Lopez, M. Casaccia, A. Paparella, *Int. J. Food Microbiol.* **2025**, *426*, 110874.
[13] M. Cáceres, W. Hidalgo, E. Stashenko, R. Torres, C. Ortiz, *Antibiotics* **2020**, *9*, 147.
[14] A. Ivanova, K. Ivanova, L. Fiandra, P. Mantecca, T. Catelani, M. Natan, E. Banin, G. Jacobi, T. Tzanov, *Int. J. Mol. Sci.* **2022**, *23*, 7527.
[15] W. C. Hsieh, C. P. Chang, Y. L. Gao, *Colloids Surf., B* **2006**, *53*, 209.
[16] K. Ivanova, A. Ivanova, E. Ramon, J. Hoyo, S. Sanchez-Gomez, T. Tzanov, *ACS Appl. Mater. Interfaces* **2020**, *12*, 35918.
[17] K. Ivanova, E. Ramon, A. Ivanova, S. Sanchez-Gomez, T. Tzanov, *Antioxidants* **2023**, *12*, 432.
[18] C. Chifiriuc, V. Grumezescu, A. M. Grumezescu, C. Saviuc, V. Lazăr, E. Andronescu, *Nanoscale Res. Lett.* **2012**, *7*, 209.
[19] A. N. Venancio, M. J. Silva, L. A. Parreira, A. A. Júlio, G. R. Souza, M. F. Conceição Santos, L. Menini, *Nat. Prod. Res.* **2024**, *0*, 1.
[20] E. Takai, A. Hirano, K. Shiraki, *J. Biochem.* **2011**, *150*, 165.
[21] M. Delfanian, M. A. Sahari, M. Barzegar, H. Ahmadi Gavlighi, F. J. Barba, *Food Chem.* **2023**, *413*, 135618.
[22] S. T. T. Pérez Rafael, K. Ivanova, G. Ferreres Cabanes, A. G. Morena, *Method to produce in situ self-assembled multifunctional nanocomposite hydrogel and its uses thereof* **2020**, EP203831508.
[23] P. Singha, J. Locklin, H. Handa, *Acta Biomater.* **2017**, *50*, 20.
[24] F. Pardini, Á. Iregui, P. Faccia, J. Amalvy, A. González, L. Irusta, *Int. J. Polym. Anal. Charact.* **2021**, *26*, 497.
[25] R. Humphries, A. M. Bobenchik, J. A. Hindler, A. N. Schuetz, *J. Clin. Microbiol.* **2021**, *59*, 12.
[26] T. Morohoshi, M. Kato, K. Fukamachi, N. Kato, T. Ikeda, *FEMS Microbiol. Lett.* **2008**, *279*, 124.
[27] E. H. James, A. M. Edwards, S. Wigneshweraraj, *FEMS Microbiol. Lett.* **2013**, *349*, 153.
[28] D. Kępińska, A. Budniak, K. Kijewska, G. J. Blanchard, M. Mazur, *Polymer (Guildf)* **2013**, *54*, 4538.
[29] Y. Ge, Y. Zhang, S. He, F. Nie, G. Teng, N. Gu, *Nanoscale Res. Lett.* **2009**, *4*, 287.
[30] A. Puertas-segura, A. G. Morena, P. Silvia, K. Ivanova, I. Ivanov, K. Todorova, P. Dimitrov, G. Ciardelli, T. Tzanov, *ACS Appl. Mater. & Interfaces* **2024**, *16*, 39129.
[31] İ. Gulcin, S. H. Alwasel, *Processes* **2023**, *11*, 2248.
[32] S. Tian, L. Shi, Y. Ren, H. C. van der Mei, H. J. Busscher, *Biofilm* **2024**, *7*, 100188.
[33] M. P. Richards, W. Chaiyasit, D. J. McClements, E. A. Decker, *J. Agric. Food Chem.* **2002**, *50*, 1254.
[34] S. C. Owen, D. P. Y. Chan, M. S. Shoichet, *Nano Today* **2012**, *7*, 53.

© 2025 The Author(s). Advanced Materials Interfaces published by Wiley-VCH GmbH

21967350, 2025, 13, Downloaded from https://advanced.onlinelibrary.wiley.com/doi/10.1002/admi.202401016 by Politecnico Di Torino Sist. Bibl Del Polit Di Torino, Wiley Online Library on [24/10/2025]. See the Terms and Conditions (https://onlinelibrary.wiley.com/terms-and-conditions) on Wiley Online Library for rules of use; OA articles are governed by the applicable Creative Commons License

[35] L. E. Nicolle, *Clin. Infect. Dis. Second Ed.* **2015**, *26*, 13.
[36] I. Kubo, K. Fujita, K. Nihei, N. Masuoka, *Bioorganic & Medicinal Chemistry* **2003**, *11*, 573.
[37] B. Kim, J. S. ParK, H. Y. Choi, J. H. Kwak, W. G. Kim, *Sci. Rep.* **2019**, *9*, 7741.
[38] M. Rayan, S. A. Lafi, M. Falah, T. Kacergius, A. Kirkliauskiene, V. Gabe, A. Rayan, *Molecules* **2023**, *28*, 1751.
[39] J. M. Costa, A. F. de Almeida Neto, *Ultrason. Sonochem.* **2020**, *68*, 105193.
[40] R. Chen, K. Zhang, Y. Shi, R. Ettelaie, Y. Shi, D. Li, S. Zhang, Y. Dang, J. Chen, *ACS Appl. Mater. Interfaces* **2024**, *16*, 19571.
[41] N. Liu, S. Ni, H. Gao, Y. Chang, Y. Fu, W. Liu, M. Qin, *Biomacromolecules* **2021**, *22*, 4501.
[42] K. Szafran, M. Jurak, A. E. Wiącek, *Colloids Surfaces A Physicochem. Eng. Asp.* **2022**, *652*, 129843.
[43] R. Teixeira-santos, L. C. Gomes, F. J. M. Mergulhão, *Curr. Opin. Biomed. Eng.* **2022**, *22*, 100394.
[44] P. Khandelwal, S. N. Abraham, G. Apodaca, *Am. J. Physiol. Physiol.* **2024**, *297*, F1477.
[45] J. Konesan, K. H. Moore, K. J. Mansfield, L. Liu, *Pathog. Dis.* **2024**, *82*, ftae026.
[46] L. Li, Y. Li, J. Yang, X. Xie, H. Chen, *Front. Immunol.* **2022**, *13*.
[47] A. M. Omer, B. Y. Eweida, T. M. Tamer, H. M. A. Soliman, S. M. Ali, A. A. Zaatot, M. S. Mohy-Eldin, *Sci. Rep.* **2021**, *11*, 19879.
[48] H. Yin, Z. Yuanrong, Y. Li, X. Zijing, J. Yongli, D. Yun, W. Danfeng, Z. Yu, *Food Packag. Shelf Life* **2022**, *41*, 101233.
[49] H. C. Lai, S. N. Chang, H. C. Lin, Y. L. Hsu, H. M. Wei, C. C. Kuo, K. P. Hwang, H. Y. Chiang, *J. Microbiol. Immunol. Infect.* **2021**, *54*, 290.

© 2025 The Author(s). Advanced Materials Interfaces published by Wiley-VCH GmbH

21967350, 2025, 13, Downloaded from https://advanced.onlinelibrary.wiley.com/doi/10.1002/admi.202401016 by Politecnico Di Torino Sist. Bibl Del Polit Di Torino, Wiley Online Library on [24/10/2025]. See the Terms and Conditions (https://onlinelibrary.wiley.com/terms-and-conditions) on Wiley Online Library for rules of use; OA articles are governed by the applicable Creative Commons License